

ELECTRON ENERGY LOSSES IN CYLINDRICAL CAVITIES: NONLOCAL EFFECTS

J. Aizpurua* and E. Uranga

Departamento de Física de Materiales, Facultad de Química, Universidad del País Vasco/
Euskal Herriko Unibertsitatea, Apto. 1072, 20080 San Sebastian, Spain

(Received for publication May 14, 1996 and in revised form November 4, 1996)

Abstract

In the framework of the dielectric theory, we present the electron energy loss probability distribution calculated for a fast probe near cylindrical surfaces using a non-local dielectric function. The small size of the drilled holes in experiments and electron trajectories close to the interface make necessary the introduction of dispersion effects when describing the energy loss spectra. We compare the results to those given by the local Drude model. The k -dependence of the dielectric function allows us to discuss energy losses in inhomogeneous media when using an effective medium dielectric function.

Key Words: Cylindrical cavities, dielectric theory, dispersion effects, electron energy losses, scanning transmission electron microscopy, semiclassical infinite-barrier, specular scattering.

Introduction

In the last decade, many microstructural systems have been studied with scanning transmission electron microscopy (STEM), which can provide high resolution transmission images and energy loss spectra (EELS). A well focused 100 keV electron beam - 0.5 nm wide - is used to obtain loss spectra with resolution as small as 0.1 eV (Ouyang *et al.*, 1992). Some quantal theories have been developed to study this kind of spectra in simple cases (Kohl, 1983; Echenique *et al.*, 1987; Ritchie and Howie, 1988), but a classical treatment has proven to be a useful tool in studying the energy loss spectra (Marks, 1982; Howie and Milne, 1985). Ritchie (1981) and Ritchie and Howie (1988) provided the link between both theories. These authors showed that quantal effects in STEM can be studied by convoluting the loss spectra of classical electrons over the lateral profile of the beam.

Many different geometries have been studied in the framework of the dielectric theory, where the electron is assumed to be a classical point particle, and excitations in the medium are described through a local dielectric function $\epsilon(\omega)$. These include planar interfaces (Ritchie, 1957; Echenique and Pendry, 1975), spheres (Ferrell and Echenique, 1985), spheroids (Illman *et al.*, 1988), edges (García-Molina *et al.*, 1985), hemispheres (Aizpurua *et al.*, 1996), coupled spheres (Schmeits and Dambly, 1991) and one sphere coupled to a planar interface (Rivacoba *et al.*, 1992; Zabala and Rivacoba, 1993). Because of the high velocity and small scattering angles of electrons in STEM most of these studies, which neglect the transferred momentum, appear to be a good approximation and have successfully described many features of the observed experimental data (Batson, 1982).

Chu *et al.* (1984) performed the first theoretical study of the energy loss of charged particles in cylindrical channels and obtained non-retarded expressions. Ashley and Emerson (1974) gave the dispersion relation for surface plasmons on cylindrical surfaces, and De Zutter and De Vleeschauwer (1986) studied the retarded expression in the axial trajectory of the electron. Excitation of surface plasmons in cylinders has been studied by other authors (Pfeiffer *et al.*, 1974; Martinos and Economou, 1981; Warmack *et al.*, 1984; Zabala *et al.*, 1989; Rivacoba *et al.*, 1995) and also the coupling between two cylinders (Schmeits, 1989). The interest on this particular

*Address for correspondence:

Javier Aizpurua

Euskal Herriko Unibertsitatea

Materia Kondentsatuaren Fisika Saila

P.K. 644, Bilbo 48080, Spain

Telephone number: +34-94-6012473

E-mail: wmpaiirj@lg.ehu.es

geometry arises from the ability of the electron beam to drill holes in some inorganic materials (Mochel *et al.*, 1983; Scheinfein *et al.*, 1985; Macaulay *et al.*, 1989; Walsh, 1989).

As the interest in interface effects and delocalization of EELS increases, larger scattering angles of the energetic incident beam have been also used in electron microscopy. This requires higher values of the transferred momentum and forces one to consider a dispersive dielectric function $\epsilon(\mathbf{k}; \vec{r}, \omega)$ to describe the medium. Non-local effects have been largely studied in the planar case. Johnson and Rimbey (1976) showed different features of spatial dispersion of an interface in terms of the additional boundary conditions (ABCs). Echenique *et al.* (1981) defined a surface dielectric function of a semi-infinite, plane-bounded metal in order to compute the image potential at points outside the surface. Fuchs and Barrera (1981) described the response of a dipole near the surface of a metal accounting for non-locality of its response, and Batson (1983) studied non-local effects in STEM, introducing dispersion effects by substituting the bulk \mathbf{k} -dependent dielectric function in the classically derived expressions. Echenique (1985) and Zabala and Echenique (1990) computed dispersion effects in the excitation of interfaces by fast electron beams and concluded that they are important when the beam travels closer than 0.5 nm to the interface. García de Abajo and Echenique (1992a,b) analysed the wake potential in a thin foil and in the vicinity of a surface of a dispersive medium.

In these latter works, the medium (usually a metal) is described with the specular scattering or semiclassical infinite-barrier (SCIB) model (Ritchie and Marusak, 1966; Fuchs and Kliewer, 1969). Although this model does not describe the diffuse nature of the metal surface, it includes the main features of non-locality. This model was applied by Dasgupta and Fuchs (1981) to study the response of a non-local sphere and was completed (Fuchs and Claro, 1987) with a multipolar expression. Rojas *et al.* (1988) introduced nonlocality to study the response of a small coated sphere.

Some recent experiments by Walsh (1989) make an interesting study of energy losses in small cylindrical holes created by the beam itself after spending some time in a fixed position on the sample. These experiments were performed in AlF_3 , which can suffer chemical change in its composition with the formation of colloidal aluminium particles when irradiating the sample with the beam. Howie and Walsh (1991) showed that these results could be explained by phenomenological extension of the Maxwell Garnett (1904) effective medium theory based on an average over electron trajectories. Expressions for the energy loss in holes with a metallic coating have been reported by Zabala *et al.* (1989), but the colloidal nature of the metallic inclusions seems to be better described through an effective medium theory as proposed by Howie and Walsh (1991). Barrera and Fuchs (1995) put this theory on more rigorous footing with a calculation of the inverse of the longitudinal dielectric function

$\epsilon^{-1}(\mathbf{k}, \omega)$ or a randomly arranged assembly of interacting spheres. This function is written in terms of a spectral representation and the \mathbf{k} -dependence is crucial to describe accurately the bulk-spectra in the system.

As the study of energy loss spectra in such a material should include a description of dispersion effects in media with cylindrical cavities, we present here the theoretical energy loss probability per unit length of a fast electron in a cavity surrounded by a standard homogeneous medium characterized by a non-local $\epsilon(\mathbf{k}, \omega)$. We will follow a scheme analogous to the one used by Dasgupta and Fuchs (1981) in the spherical case, assuming the SCIB to be valid to describe the medium response.

Once the expressions for cylindrical cavities are obtained, we discuss the possibility of their application to more complicated inhomogeneous media, such as those characterized by an effective \mathbf{k} -dependent response function, or to microstructures such as tubular fullerenes.

Non-local Expressions for the Potential in a Cavity

We first define the Fourier transformations in space and time that we use

$$f(\vec{r}, t) = \frac{1}{(2\pi)^4} \int_{-\infty}^{+\infty} d^3\vec{k} \int_{-\infty}^{+\infty} d\omega f(\vec{k}, \omega) e^{i\vec{k}\vec{r}} e^{-i\omega t} \quad (1)$$

and its inverse:

$$f(\vec{k}, \omega) = \int_{-\infty}^{+\infty} d^3\vec{r} \int_{-\infty}^{+\infty} dt f(\vec{r}, t) e^{-i\vec{k}\vec{r}} e^{i\omega t} \quad (2)$$

We use atomic units throughout this paper.

Let us assume that an electron is moving in a cylindrical hole of radius a , parallel to the Z -axis, with velocity v at a distance ρ_0 from the centre of the holes as shown in Figure 1. The material is characterized by a dielectric function $\epsilon(\mathbf{k}, \omega)$, and retardation effects are neglected as the cavity is assumed to be smaller than the wavelength of light. The Laplace equation can be separated in cylindrical coordinates in a standard way, and Poisson's equation can be solved through an expansion of Green functions in cylindrical coordinates (Jackson, 1962). The potential $V(\mathbf{r}; \vec{r})$ inside the cylinder (as-sumed to be the vacuum) is then given by:

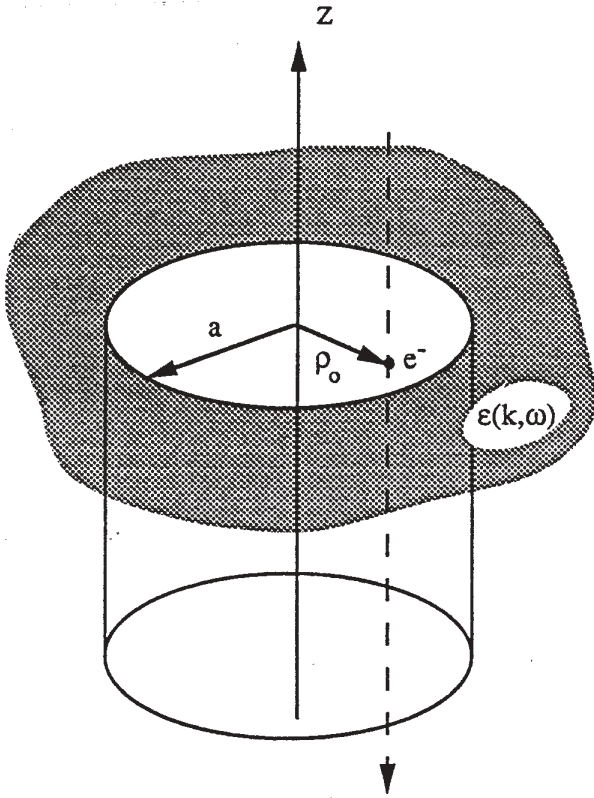


Figure 1. Electron moving in a hole parallel to the cylinder axis with velocity v at a distance ρ_0 from the centre of the cylinder of radius a . The surrounding medium is characterized by a non-local dielectric function $\epsilon(\mathbf{k}, \omega)$.

$$V(\vec{r}, \omega) = \frac{-1}{2\pi} \int_{-\infty}^{+\infty} dq e^{iqz} \sum_{m=-\infty}^{+\infty} \{4\pi\delta(\omega - qv) e^{im\phi} [I_m(q\rho_0)K_m(q\rho)\theta(\rho - \rho_0) + K_m(q\rho_0)I_m(q\rho)\theta(\rho_0 - \rho)]\} + \frac{1}{2\pi} \int_{-\infty}^{+\infty} dq e^{iqz} \sum_{m=-\infty}^{+\infty} A_m e^{im\phi} I_m(q\rho) \quad (3)$$

where the first term is the direct Coulomb term, and the second one is the induced term which has to be obtained by imposing the standard boundary conditions, i.e., the continuity of the potential and the normal component of the displacement at $\rho = a$. $I_m(x)$ and $K_m(x)$ are the modified Bessel functions of order m (Gradshteyn and Ryzkik, 1963) and $\theta(x)$ is the Heaviside function. Therefore, the problem reduces to finding the A_m coefficients in the induced term of the potential.

Outside the cavity ($\rho > a$) we can write

$$\vec{\nabla} \cdot \vec{D} = 0 \quad (4a)$$

$$\vec{\nabla} \times \vec{E} = 0 \quad (4b)$$

Following Ritchie and Marusak (1966), we will assume an infinite fictitious medium in order to solve for the fields outside the cylinder. This medium satisfies the following conditions: (i) Maxwell's equations are continued to the $\rho > a$ region of the infinite medium; (ii) the fields outside the real cylinder are the same as the ones of the infinite medium with the same response function; (iii) the normal component of the displacement D_ρ is discontinuous in $\rho = a$ in this infinite system, but the tangential components are continuous.

Therefore, we introduce a uniform dielectric medium with a fictitious cylinder of charge at $\rho = a$, which acts as a source for D . Because of this, (which normally holds throughout an infinite, continuous medium) $\vec{\nabla} \cdot \vec{D} = 0$ does not hold on the surface of the cylinder.

We introduce now the potential function $V_D(\mathbf{r}; \rightarrow)$ defined by

$$\vec{D}(\vec{r}) = -\vec{\nabla} V_D(\vec{r}) \quad (5)$$

We note that inside the cylinder of the fictitious medium $V(\mathbf{r}; \rightarrow)$ and $V_D(\mathbf{r}; \rightarrow)$ must be of the form:

$$V(\vec{r}) = \frac{1}{2\pi} \int_{-\infty}^{+\infty} dq e^{iqz} \sum_{m=-\infty}^{+\infty} e^{im\phi} \tilde{V}_m(\rho) \quad (6)$$

$$V_D(\vec{r}) = \frac{1}{2\pi} \int_{-\infty}^{+\infty} dq e^{iqz} \sum_{m=-\infty}^{+\infty} e^{im\phi} \tilde{V}_{Dm}(\rho) \quad (7)$$

Equations (4) and (5) reduce to

$$\nabla^2 V_D = 0 \quad (8)$$

Multiplying by $\exp(-ik; \rightarrow \bullet \mathbf{r}; \rightarrow)$ and integrating we get:

$$-k^2 V_D(\vec{k}) + a \sum_{m=-\infty}^{+\infty} \frac{1}{2\pi} C_m \left[\int_{-\infty}^{+\infty} dz \int_0^{2\pi} d\phi e^{-i\vec{k}\vec{r}} \int_{-\infty}^{+\infty} dq e^{iqz} e^{im\phi} \right]_{\rho=a} = 0 \quad (9)$$

with

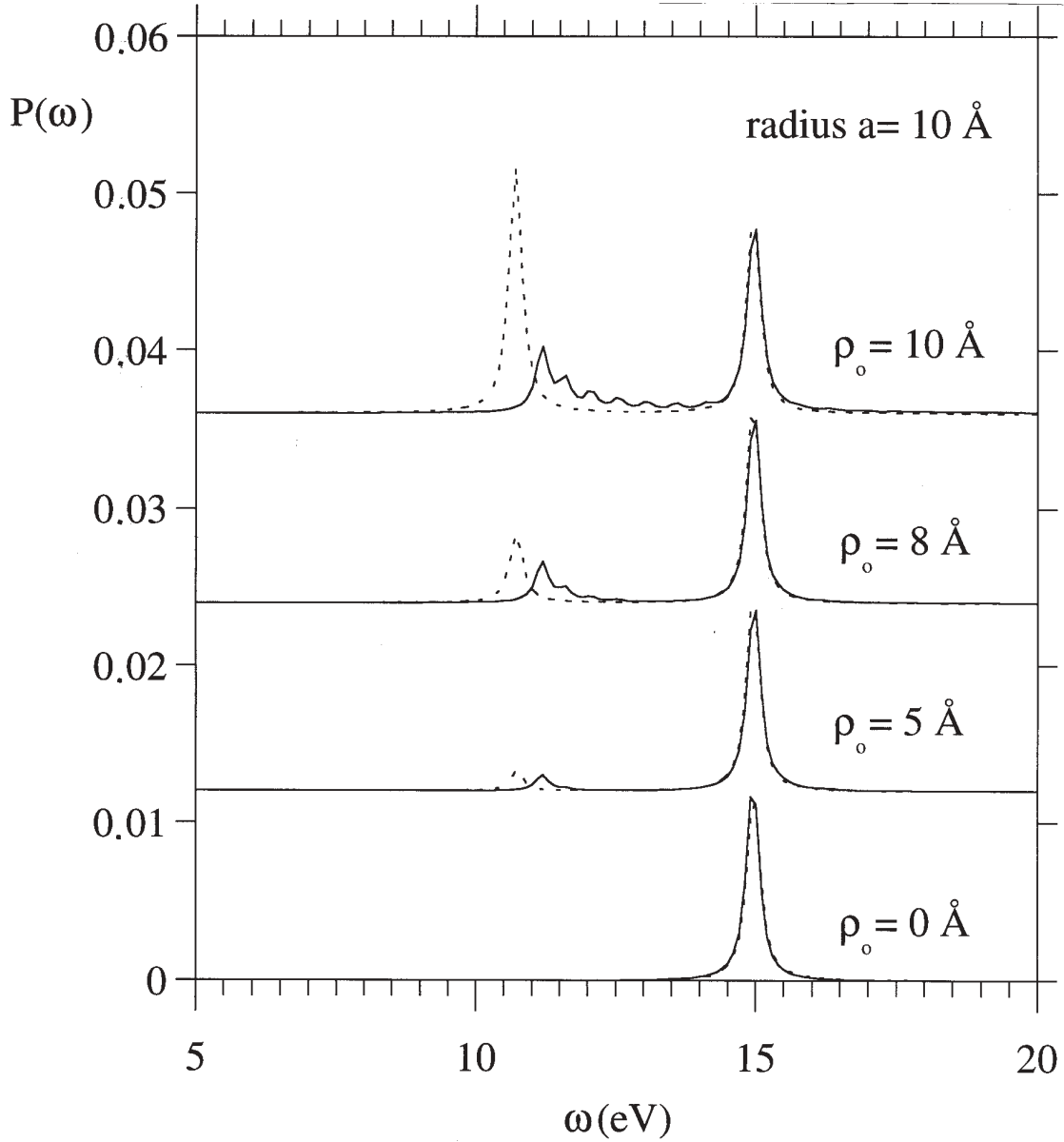


Figure 2. Energy loss probability per unit length $P(\omega)$ for an electron passing through a 10 Å radius hole in Al at different distances from the centre of the hole. Dashed lines show the spectra of losses when using a local dielectric function, and the solid lines show the spectra of losses when using a non-local dielectric function given by the hydrodynamical model. $\omega_p = 15.1$ eV and $\gamma = 0.1\omega_p$. The spectra have been displaced vertically.

$$C_m = -\left[\frac{d\tilde{V}_{Dm}}{d\rho}\right]_{\rho=a^-} + \left[\frac{d\tilde{V}_{Dm}}{d\rho}\right]_{\rho=a^+} \quad (10)$$

$$e^{-i\vec{k}\vec{r}} = e^{-iqz} \sum_{p=-\infty}^{+\infty} (-i)^p e^{ip(\theta-\phi)} J_p(Q\rho) \quad (11)$$

We expand $\exp(-i\vec{k}\cdot\vec{r})$ in cylindrical coordinates by using the relation (Jackson, 1962):

where $k^2 = Q^2 + q^2$ and θ and ϕ are the azimuthal angles of \vec{k} ; \vec{r} and \vec{r} ; \vec{r} respectively and $J_p(Q\rho)$ is the Bessel function of order p .

After integrating eq. (9) over z and φ we get:

$$V_D(\vec{k}, \omega) = \sum_{m=-\infty}^{+\infty} 2\pi a C_m (-i)^m e^{im\theta} \frac{J_m(Qa)}{Q^2 + q^2} \quad (12)$$

whence

$$V(\vec{k}, \omega) = \sum_{m=-\infty}^{+\infty} 2\pi a C_m (-i)^m e^{im\theta} \frac{J_m(Qa)}{(Q^2 + q^2)\varepsilon(\vec{k}, \omega)} \quad (13)$$

We come back to the space coordinate using eq. (1) and obtain:

$$V_D(\vec{r}, \omega) = \frac{a}{(2\pi)^2} \sum_{m=-\infty}^{+\infty} C_m e^{im\varphi} \int_{-\infty}^{+\infty} dq e^{iqz} \int_0^{+\infty} QdQ \frac{J_m(Qa)J_m(Q\rho)}{Q^2 + k_z^2} \quad (14)$$

and

$$V(\vec{r}, \omega) = \frac{a}{(2\pi)^2} \sum_{m=-\infty}^{+\infty} C_m e^{im\varphi} \int_{-\infty}^{+\infty} dq e^{iqz} \int_0^{+\infty} QdQ \frac{J_m(Qa)J_m(Q\rho)}{(Q^2 + k_z^2)\varepsilon(\vec{k}, \omega)} \quad (15)$$

Now we will take these potentials as the ones of our real system outside the cylinder ($\rho > a$) and match them at $\rho = a$ with those given by eq. (3), which was valid inside the cylinder ($\rho < a$). $D_\rho(\vec{r}^+;)$ is obtained in both cases through $\vec{D}(\vec{r}) = -\vec{\nabla}\nabla V_D(\vec{r})$ and has to be also continuous at $\rho = a$. We solve equations of continuity for $V(a^+) = V(a^-)$ and $D_\rho(a^+) = D_\rho(a^-)$ and get for A_m :

$$A_m = 4\pi\delta(\omega - qv)I_m(q\rho_0)K'_m(qa) \frac{\tilde{\varepsilon}_m(q, \omega)K_m(qa)I_m(qa) - 1}{\tilde{\varepsilon}_m(q, \omega)I_m^2(qa)K'_m(qa) - I'_m(qa)} \quad (16)$$

with

$$\frac{1}{\tilde{\varepsilon}_m(q, \omega)} = \int_0^\infty \frac{J_m^2(Qa)}{(Q^2 + q^2)\varepsilon(\vec{k}, \omega)} QdQ \quad (17)$$

$$\text{where } k^2 = Q^2 + q^2$$

that can be introduced in the expression of the potential inside the cylinder to account for dispersion effects.

Electron Energy Losses in the Cavity

We study now the Electron Energy Losses (EELS) of an electron in the cavity surrounded by a material characterized by a $\varepsilon(\vec{k}, \omega)$ response function.

The probability of losing energy $\hbar\omega$ is given by the induced field evaluated at the particle point ($\rho = \rho_0$, $\varphi = \varphi_0$, $z = vt$):

$$- \left| \frac{\partial \phi_o^{ind}(\vec{r}, t)}{\partial z} \right|_{\rho=\rho_0} = \int_0^\infty d\omega \omega P(\omega) \quad (18)$$

where $\phi_o(\vec{r}, t)$ is given by the Fourier transformation of eq. (3). After some algebra, we get for the energy loss probability distribution:

$$P(\omega) = \frac{2}{\pi v^2} \sum_{m=-\infty}^{m=+\infty} I_m^2\left(\frac{\omega\rho_0}{v}\right) K'_m\left(\frac{\omega a}{v}\right) \text{Im} \left[\frac{\tilde{\varepsilon}_m(\omega)K_m\left(\frac{\omega a}{v}\right)I_m\left(\frac{\omega a}{v}\right) - 1}{\tilde{\varepsilon}_m(\omega)I_m^2\left(\frac{\omega a}{v}\right)K'_m\left(\frac{\omega a}{v}\right) - I'_m\left(\frac{\omega a}{v}\right)} \right] \quad (19)$$

with

$$\frac{1}{\tilde{\varepsilon}_m(\omega)} = \int_0^\infty \frac{J_m^2(Qa)}{(Q^2 + \frac{\omega^2}{v^2})\varepsilon(\vec{k}, \omega)} QdQ \quad (20)$$

and $\text{Im}[x]$ the imaginary part of x .

If we take $\varepsilon(\vec{k}, \omega) = \varepsilon(\omega)$, we recover the wellknown local limit,

$$P(\omega) = \frac{2}{\pi v^2} \sum_{m=-\infty}^{m=+\infty} I_m^2\left(\frac{\omega\rho_0}{v}\right) K'_m\left(\frac{\omega a}{v}\right) K_m\left(\frac{\omega a}{v}\right) \text{Im} \left[\frac{\varepsilon(\omega) - 1}{\varepsilon(\omega)I_m\left(\frac{\omega a}{v}\right)K'_m\left(\frac{\omega a}{v}\right) - I'_m\left(\frac{\omega a}{v}\right)K_m\left(\frac{\omega a}{v}\right)} \right] \quad (21)$$

In order to study the effects of dispersion, we consider the simple non-local response function of the hydrodynamic

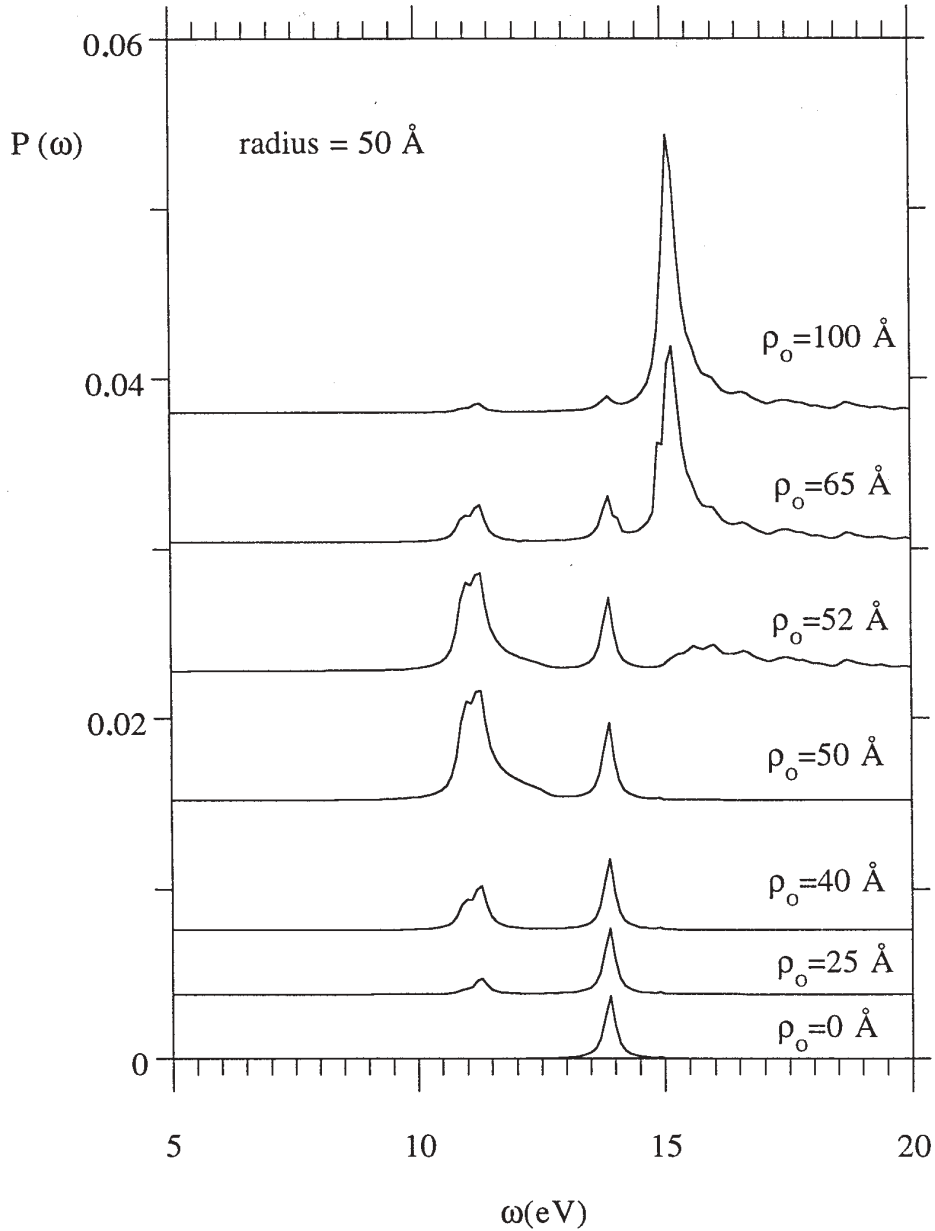


Figure 3. Energy loss probability per unit length $P(\omega)$ for an electron passing through or near a 50 Å radius hole in Al when using a non-local dielectric function to characterize the medium. Different trajectories inside and outside the hole are shown. Notice that the result at the interface itself becomes the same in a non-local treatment. $\omega_p = 15.1$ eV and $\gamma = 0.1 \omega_p$. The spectra have been displaced vertically.

model:

$$\varepsilon(k, \omega) = 1 - \frac{\omega_p^2}{\omega(\omega + i\gamma) - \beta^2 k^2} \quad (22)$$

where $\beta = 3/5v_F^2$, v_F is the Fermi velocity, ω_p is the plasmon frequency, and γ is the damping. We consider a hole in aluminium ($\omega_p = 15.1$ eV and $\gamma = 0.1 \omega_p$).

In Figure 2, the loss spectrum for a cylindrical cavity of radius $a = 10$ Å surrounded by a medium characterized by the non-local response function (solid line) is compared to

that using a local response (dashed line). There appear two peaks in the local case at 10.6 eV and 15 eV associated to the $m = 1$ and $m = 0$ modes, respectively, while in the non-local case the low energy peak ($m = 1$) shifts 0.7 eV up and appears at 11.2 eV. The $m = 0$ mode (15 eV), which is a surface mode for very small radius and not a bulk one, is not affected by dispersion effects, as it is associated to the monopolar charge distribution. This is the dominant excitation for axial trajectories and is not affected by dispersion, as it is far from the cylinder walls. At points closer to the interface, dispersion effects change the weight and position of the low energy surface losses associated to the $m = 1$ mode and make it almost disappear. This change is more noticeable when the electron is travelling along the interface itself. In a local treatment, different results are obtained when the beam approaches the interface from the inner or outer side of the cylinder, but when this problem is solved in a non-local treatment, the same result is found. As the radius of the cavity becomes larger, the low energy surface plasmon excitations are more important in weight compared to the $m = 0$ excitation. This can be observed in Figure 3, where the loss spectrum for a cylindrical cavity of radius $a = 50 \text{ \AA}$ is shown. Although dispersion effects depress the intensity and shift the position of the low energy plasmon (11.2 eV), this mode becomes comparable in magnitude to the high energy one (13.9 eV) when the electron travels close enough to the interface. This latter excitation has also shifted down in value because of the bigger radius and tends to the low energy plasmon value as the radius becomes larger. It will join the low energy plasmon as a planar surface plasmon in the limit of very large radius.

There is no appreciable difference in the theoretical spectra calculated using the Mermin, k -dependent, response function because momentum transfers are small, so it is sufficient to use the hydrodynamic response function here.

Possible Applications

As pointed out in the Introduction, the origin of this study was interest in the formation of cylindrical holes in some inorganic materials by the STEM electrons. The beam occupies the whole cavity as it increases in size, and it is useful to accurately model the losses experienced by non-axial electrons, which are influenced appreciably by nonlocality of the medium as shown.

We have performed this study in a homogeneous metallic system characterized by a standard hydrodynamic response function, but we should recall that some experimental data of losses in cylindrical cavities are obtained in complex inhomogeneous media (Walsh, 1989).

The k -dependent spectral representation of the effective bulk response function in AlF_3 with embedded colloidal Aluminium spheres (Barrera and Fuchs, 1995), provides the most satisfactory way of interpreting such

experimental data, so we are now facing up to the possibility of deducing an effective surface response function from the bulk response function. We can consider two approaches to this problem. We could try to obtain in a straightforward way an effective surface response function by taking the interface as another inhomogeneous feature to be taken into account. Alternatively, we could use the k -dependent effective medium bulk-response into the expressions found from the SCIB. When calculating in this way, energy losses at bulk plasmon values appear even for external trajectories of the electrons in very big holes and near planar surfaces. The legitimacy of this latter proposal is not clear and may even be quite inconsistent, as the k -dependence of the effective medium response arises from the geometrical features of the colloidal inclusions and not from the behaviour of the electron gas, as is in the case of an homogeneous medium characterized by a non-local response function which can be introduced in the SCIB.

However, when we use this spectral representation in the expressions for non-local cylinders, the agreement between experiment and theory is quite satisfactory, and this could lead us to trust the use of this model when treating inhomogeneous systems. At any rate, the limits of the SCIB for such an effective response have to be more deeply studied and corresponding results for planar surfaces better understood.

Acknowledgments

The authors wish to acknowledge Professor A. Howie and Dr. A. Rivacoba for his reading of the manuscript, and also the helpful suggestions made by the reviewers. J. Aizpurua thanks the Hezkuntza, Unibertsitate eta Ikerketa Saila, for their economical support.

References

- Aizpurua J, Rivacoba A, Apell SP (1996) Electron energy losses in hemispherical particles. *Phys. Rev.* **B54**: 2901-2909.
- Ashley JC, Emerson LC (1974) Dispersion relations for non-radiative surface plasmons on cylinders. *Surf. Sci.* **41**: 615-618.
- Barrera RG, Fuchs R (1995) Theory of the energy loss in a random system of spheres. *Phys. Rev.* **B52**: 3256-3273.
- Batson PE (1982) Surface plasmon coupling in clusters of small spheres. *Phys. Rev. Lett.* **49**: 936-940.
- Batson PE (1983) Surface plasmon scattering on flat surfaces at grazing incidence. *Ultramicroscopy* **11**: 299.
- Chu YT, Warmack RJ, Ritchie RH, Little JW, Becher RS, Ferrell TL (1984) Contribution of the surface plasmon to energy losses by electrons in cylindrical channel. *Particle Accelerators* **16**: 13-17.

- Dasgupta BB, Fuchs R (1981) Polarizability of a small sphere including nonlocal effects. *Phys. Rev.* **B24**: 554-561.
- De Zutter D, De Vleeschouwer D (1986) Radiation from and forces acting on a point charge moving through a cylindrical hole in a conducting medium. *J. Appl. Phys.* **59**: 4146-4150.
- Echenique PM, Pendry JB (1975) Absorption profile at surfaces. *J. Phys.* **C8**: 2938-2942.
- Echenique PM, Ritchie RH, Barberán N, Inkson J (1981) Semiclassical image potential at a solid surface. *Phys. Rev.* **B23**: 6486-6492.
- Echenique PM (1985) Dispersion effects in the excitation of interfaces by fast-electron beams. *Phil. Mag.* **B52**: L9-L13.
- Echenique PM, Bausells J, Rivacoba A (1987) Energy-loss probability in electron microscopy. *Phys. Rev.* **B35**: 1521-1524.
- Ferrell TL, Echenique PM (1985) Generation of surface excitations on dielectric spheres by an external electron beam. *Phys. Rev. Lett.* **55**: 1526-1529.
- Fuchs R, Kliever KL (1969) Optical properties of an electron gas: Further studies of a nonlocal description. *Phys. Rev.* **185**: 905-913.
- Fuchs R, Barrera RG (1981) Dynamical response of a dipole near the surface of a nonlocal metal. *Phys. Rev.* **B24**: 2940-2950.
- Fuchs R, Claro F (1987) Multipolar response of small metallic spheres: Nonlocal theory. *Phys. Rev.* **B35**: 3722-3727.
- García de Abajo FJ, Echenique PM (1992) Wake-potential formation in a thin foil. *Phys. Rev.* **B45**: 8771-8774.
- García de Abajo FJ, Echenique PM (1992) Wake potential in the vicinity of a surface. *Phys. Rev.* **B46**: 2663-2675.
- García-Molina R, Gras-Marti A, Ritchie RH (1985) Excitation of edge modes in the interaction of electron beams with dielectric wedges. *Phys. Rev.* **B31**: 121-126.
- Gradshteyn IS, Ryzhik IM (1963) *Table of Integral, Series and Products*. 4th edition. Translated by A. Jeffrey. Academic Press, New York. p. 967.
- Howie A, Milne RH (1985) Excitations at interfaces and small particles. *Ultramicroscopy* **18**: 427-434.
- Howie A, Walsh CA (1991) Interpretation of valence loss spectra from composite media. *Microsc. Microanal.* **2**: 171-181.
- Illman BL, Anderson VE, Warmack RJ, Ferrell TL (1988) Spectrum of surface-mode contributions to the differential energy-loss probability for electrons passing by a spheroid. *Phys. Rev.* **B38**: 3045-3049.
- Jackson JD (1962) *Classical Electrodynamics*. 2nd Edn. John Wiley & Sons, New York. pp. 102-108, 116-118, 131.
- Johnson DL, Rimbey PR (1976) Aspects of spatial dispersion in the optical properties of a vacuum-dielectric interface. *Phys. Rev.* **B14**: 2398-2410.
- Kohl H (1983) Image formation by inelastically scattered electrons: Image of a surface plasmon. *Ultramicroscopy* **11**: 53-65.
- Macaulay JM, Allen RM, Brown LM, Berger SD (1989) Nanofabrication using inorganic resists. *Microelectron. Eng.* **9**: 557-560.
- Marks LD (1982) Observation of the image force for fast electrons near an MgO surface. *Solid State Comm.* **43**: 727-729.
- Martinos SS, Economou EN (1981) Excitation of surface plasmons in cylinders by electrons. *Phys. Rev.* **B24**: 6908-6914.
- Maxwell Garnett JC (1904) Colours in metal glasses and in metallic films. *Phil. Trans. Roy. Soc.* **203**: 385-420.
- Mochel ME, Humphreys CJ, Eades JA, Mochel JM, Petford AK (1983) Electron beam writing on a 20-Å scale in metal β -aluminas. *Appl. Phys. Lett.* **42**: 392-394.
- Ouyang F, Batson PE, Isaacson M (1992) Quantum size effects in the surface plasmon-excitation of small metallic particles by electron-energy-loss-spectroscopy. *Phys. Rev.* **B46**: 15421-15425.
- Pfeiffer CA, Economou EN, Ngai KL (1974) Surface polaritons in a circularly cylindrical interface: Surface plasmons. *Phys. Rev.* **B10**: 3038-3051.
- Ritchie RH (1957) Plasma losses by fast electrons in thin films. *Phys. Rev.* **106**: 874-881.
- Ritchie RH (1981) Quantal aspects of the spatial resolution of energy-loss measurements in electron microscopy. I. Broadbeam geometry. *Philos. Mag.* **A44**: 931-942.
- Ritchie RH, Howie H (1988) Inelastic scattering probabilities in scanning transmission electron microscopy. *Philos. Mag.* **A58**: 753-767.
- Ritchie RH, Marusak AL (1966) The surface plasmon dispersion relation for an electron gas. *Surf. Sci.* **4**: 234-240.
- Rivacoba A, Zabala N, Echenique PM (1992) Theory of energy loss in scanning transmission electron microscopy of supported small particles. *Phys. Rev. Lett.* **69**: 3362-3365.
- Rivacoba A, Apell P, Zabala N (1995) Energy loss probability of STEM electrons in cylindrical surfaces. *Nucl. Instr. Meth.* **B96**: 465-469.
- Rojas R, Claro F, Fuchs R (1988) Nonlocal response of a small coated sphere. *Phys. Rev.* **B37**: 6799-6807.
- Scheinfel M, Muray A, Isaacson M (1985) Electron energy loss spectroscopy across a metal-insulator interface at sub-nanometer spatial resolution. *Ultra-microscopy* **16**: 233-239.
- Schmeits M (1989) Surface-plasmon coupling in cylindrical pores. *Phys. Rev.* **B39**: 7567-7577.
- Schmeits M, Dambly L (1991) Fast-electron scattering by bispherical surface-plasmon modes. *Phys. Rev.* **B44**: 12706-12712.
- Walsh CA (1989) Analysis of electron energy-loss

spectra from electron-beam-damaged amorphous AlF_3 . *Phil. Mag.* **A59**: 227-246.

Warmack RJ, Becker RS, Anderson VE, Ritchie RH, Chu YT, Little J, Ferrell TL (1984) *Phys. Rev.* **B29**: 4375.

Zabala N, Echenique PM (1990) Energy loss of fast electrons moving near plane boundaries with dispersive media. *Ultramicroscopy* **32**: 327-335.

Zabala N, Rivacoba A (1993) Electron energy loss near supported particles. *Phys. Rev.* **B48**: 14534-14542.

Zabala N, Rivacoba A, Echenique PM (1989) Energy loss of electrons travelling through cylindrical holes. *Surf. Sci.* **209**: 465-480.

Discussion with Reviewers

P.E. Batson: In Figure 3, the $Q = 0$ bulk mode is depressed within about 10 \AA of the cylinder walls. Can you briefly discuss the lateral extent of the bulk plasmon charge density disturbance when the probe electron travels close to the small cylinder? Does the proximity of a convex object to one side of the probe confine the plasmon fluctuation to a small volume surrounding the probe?

Authors: As in the case of a planar interface, two effects take place when the beam travels close enough to a boundary: the creation of surface plasmon losses and on the other hand, a decrease in the probability of losing energy at the bulk plasmon energy (what is known as “Begrenzung”). The cylindrical case is analogous to the planar one in the sense that, as the beam gets closer to the interface, the bulk plasmon fluctuation is confined and disappears when the beam travels along the interface. This effect is not only associated with convex objects which can confine the fluctuation, but also with any other kind of boundaries, as in the case of the planar one. As pointed out by the reviewer, this confinement can be noticeable from about 10 \AA for Al.

R.H. Ritchie: The calculations presented have been made using specular reflection condition (or SCIB) and finally, the simple hydrodynamical dielectric function was employed in computing the “surface dielectric function” from SCIB theory. If the pure hydrodynamical model, together with appropriate ABCs, had been used, would appreciably different results be found?

Authors: The fact that both treatments are equivalent in the plane-bounded medium (Garcia de Abajo and Echenique, 1992) leads us to think that it could also be equivalent in the cylindrical case. In any case, it would be good to study the pure hydrodynamical model in cylindrical coordinates in order to be absolutely sure of the equivalence.

R.H. Ritchie: Why are no losses at energies corresponding to $m = 2$ and greater observable in the local dielectric calculations shown in Figure 2?

Authors: They are not observable because, in a local treatment, all the modes ($m = 1, m = 2, m = 3, \dots$) appear almost at the same position (Rivacoba *et al.*, 1995). In this way, the intensity of the peak at 10.6 eV , when using a local dielectric function, is due to the contribution of many modes (mainly $m = 1, m = 2$ and $m = 3$). High modes are not correctly treated by a local response function in the sense that it neglects correlation in the surface charge fluctuations. This correlation seems to be more important in larger m modes which involve greater charge fluctuations. Therefore, when dispersion effects are introduced, these modes are shifted up and spread into smaller peaks in different positions. It is possible then to identify each mode as a m mode.

R.H. Ritchie: The authors state that their loss spectrum computed using a local dielectric function, for a trajectory coincident with the interface, differs depending whether the trajectory approaches the interface from larger or from smaller values. Why is this? In the case of the plane-bounded medium, such discrepancies may be eliminated by proper choice of the cutoff wave number.

Authors: Yes, you are right. Instead of saying that different values are found in a local treatment, we could say that in a local treatment, a proper cutoff must be chosen in order to get the same result when the beam approaches the interface from the inner or from the outer side of the cylinder, while the same result is found in a straightforward way in a non-local treatment.